

See discussions, stats, and author profiles for this publication at: <https://www.researchgate.net/publication/224026237>

Multiwave imaging and super resolution

Article in *Physics Today* · February 2010

DOI: 10.1063/1.3326986

CITATIONS

69

READS

1,009

2 authors, including:



Mickaël Tanter

École Supérieure de Physique et de Chimie Industrielles

600 PUBLICATIONS 17,270 CITATIONS

[SEE PROFILE](#)

Some of the authors of this publication are also working on these related projects:



Beta-catenin Dependent Oncogenic Mechanical Induction in Cancer progression, in vivo. [View project](#)



transcranial brain therapy [View project](#)

Multiwave imaging and super resolution

Mathias Fink and Mickael Tanter

Interactions between different kinds of waves can yield medical images that beat the single-wave resolution limit.

Mathias Fink is director of the Langevin Institute at the École Supérieure de Physique et de Chimie Industrielles de la Ville de Paris in Paris. **Mickael Tanter** is a research professor in the institute. They, along with six others, founded SuperSonic Imagine in 2005.

The human body supports the propagation of many kinds of waves, each of which can provide an image with a specific type of information. For example, ultrasonic waves reveal a tissue's density and how it responds to compression forces, and mechanical shear waves indicate how tissues respond to shear forces. Low-frequency electromagnetic waves are sensitive to electrical conductivity; optical waves tell about optical absorption. In all those circumstances, physicists have striven to obtain the best overall contrast and resolution. Now, after decades of work, we are pushing against the physical limits inherent in each imaging modality. As described in the box on page 30, that limit is, in many cases, *not* determined by wavelength.

Physicians quickly realized that for medical imaging and diagnosis, one way to overcome the inherent limits of single-mode imaging is to combine different imaging modalities. The basic idea of multimodality imaging—for example, in the combination of positron emission tomography and computed tomography—is to associate the high-resolution morphological image of a first modality (CT) to an image of the second modality (PET) that is poorly resolved but that provides a clinically interesting contrast, revealing metabolic activity in this case. A second example of multimodality imaging, used for mammography, combines ultrasound and x-ray images. However, multimodality imaging remains extremely costly and constrained by the inherent physical limits of each separate imaging mode.

New approaches

Is there any way to improve diagnostic capabilities other than with multimodality imaging? Two scientific communities have suggested new research directions. One line of attack, called molecular imaging, was proposed by chemists and biologists. It differs from traditional imaging in that biomarkers are used to help image particular targets or pathways. Those biomarkers interact chemically with their surroundings and thereby increase the contrast.

The other approach was proposed independently by various groups in the physics community. It consists of combining two different waves—one to provide contrast, another to provide spatial resolution—to build a new kind of image. Because of the way the waves are combined, multiwave imaging produces a single image with the best contrast and resolution properties of the two waves. Multimodality imaging, on the other hand, relies on the analysis of two images, each limited by the contrast and resolution properties of the wave that generated it.

Three different types of wave interaction can be exploited in multiwave imaging. In one application, the interaction of one kind of wave with tissue can generate a second kind of wave. In thermoacoustic imaging, for example, absorbed electromagnetic radiation causes a transient change in temperature that radiates an ultrasonic wave through thermal expansion (see the article by Stanislav Y. Emelianov, Pai-Chi Li, and Matthew O'Donnell in *PHYSICS TODAY*, May 2009, page 34).

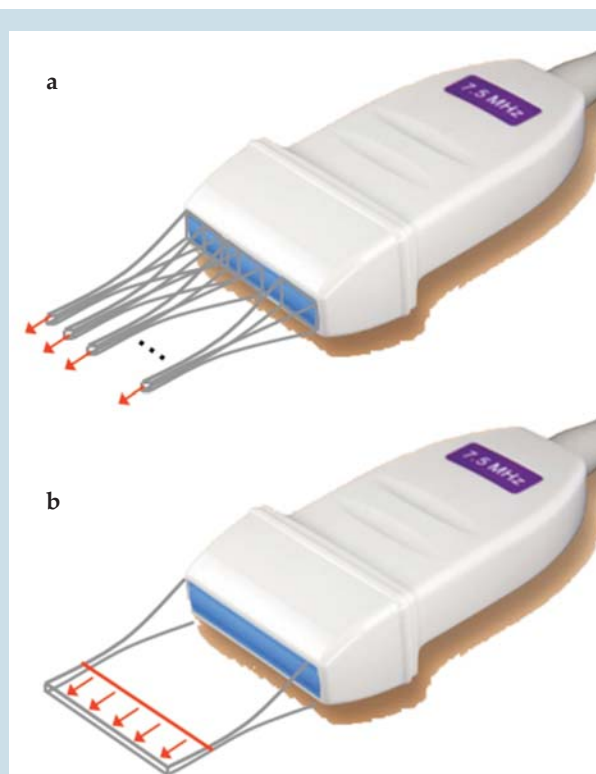


Figure 1. Conventional versus ultrafast ultrasonic imaging. **(a)** In conventional ultrasound, 100 or more beams are focused on different locations and the subsequent backscattered echoes are processed to generate a single image. **(b)** In ultrafast imaging, a plane wave probes the whole medium in a single shot. Again, the backscattered echoes are processed to produce the ultrasonic image.

In another approach, a low-resolution wave that carries information about the desired contrast can be locally modulated by a second wave that has good spatial resolution. An example is acousto-optical imaging (also called acousto-optical tomography), in which an optical beam traveling through tissue is modulated at ultrasonic frequency by a focused ultrasound beam. Demodulating the image—that is, finding the light whose frequency has been shifted—enables one to observe the photons that traveled through the ultrasonic focal spot. Steering that spot to different locations yields a complete image with a contrast mainly determined by the optical absorption and with the submillimeter resolution of the ultrasonic wave.

The third case involves waves that travel at very different speeds. The faster wave can be used to produce a movie of the slow wave propagation. In transient elastography, for instance, ultrafast ultrasonic scanners can track tissue motion induced by low-speed shear waves.

Multiwave generation and modulation

Thermoacoustic imaging and related techniques rely on a dissipative process that transforms pulsed electromagnetic energy into transient tissue motion that radiates coherent ultrasonic waves. A recording of the ultrasonic field reaching an array of piezoelectric transducers leads to an image of the ultrasound sources with the submillimeter resolution of the ultrasonic wave. Because the speed of ultrasound is about the same for all soft tissues—roughly 1500 m/s—the reconstruction process is relatively simple.

Both microwaves and optical waves have been used in thermoacoustic applications. The microwaves, which penetrate deeper, yield conductivity images; indeed, the first conductivity images of breast tissue have now been obtained via this modality. The photoacoustic approach with optical waves has been used to generate vascular images in small animals.

Magnetoacoustic tomography, a technique that may improve the spatial resolution of electrical impedance tomography, is also a modality based on a dissipative process. As described in the box, electrical impedance tomography relies on numerous electrodes placed on the skin. In magnetoacoustic tomography, tissues displaced via electric or magnetic stimulation produce ultrasound.¹ In an interesting variation based on magnetic induction, tissues are put in both a strong static magnetic field and a second field that varies with a frequency on the order of a megahertz. The time-varying magnetic field induces eddy currents in the tissue; in the presence of the static field, the tissue feels a Lorentz force that induces ultrasonic waves. In that approach, the acoustic-wave amplitude is proportional to the electrical conductivity of the tissue in the megahertz range. For a static field with a magnitude of 1 T and a typical conductivity value of 0.2 siemens/m, the radiated ultrasonic pressure field of some 10 millibars is strong enough to be measured by ultrasonic transducers.

Acousto-optic imaging, not to be confused with photoacoustic imaging, is another technique that combines ultrasound and light. As described above, ultrasound is not radiated by tissues absorbing light but rather is generated from

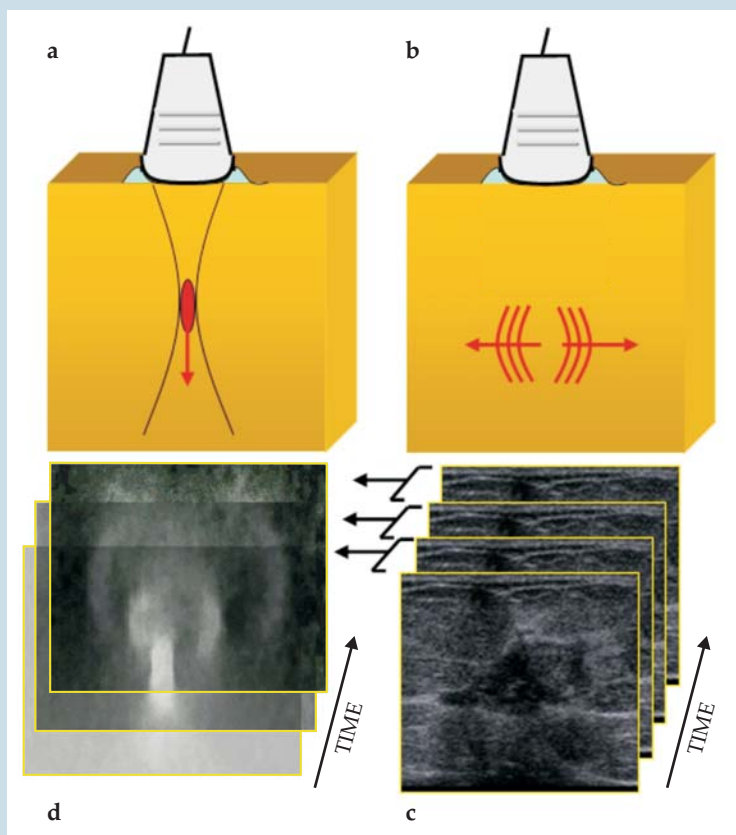


Figure 2. Elasticity imaging. (a) An ultrasonic probe generates a force in the focal area that pushes in the direction of beam propagation. (b) Relaxation of the pushed tissue generates a low-frequency shear wave. The ultrasonic array then switches into an ultrafast imaging mode. (c) Ultrasonic images, dominated by speckle patterns, are created and then stored into memories. (d) Correlation of the speckle patterns in sequential frames yields an image of the tissue displacement induced by the shear wave.

a focused transducer. With a well-controlled ultrasonic modulation of light, it is possible to recover the optical properties of tissues several centimeters deep, even though light transmitted by a laser beam loses its coherence after some hundreds of microns.

After light has been transmitted through an organ, the spatial distribution of light intensity registered by a CCD camera will show a well-known, random speckle pattern, a consequence of the interference between the light's multiple scattering paths. The part of the speckle pattern corresponding to photons that traveled through the ultrasonic focal spot will be modulated at the ultrasonic frequency. Two main mechanisms contribute to that modulation. One involves the variation of optical scattering paths due to ultrasound-induced displacements of optical scatterers. The second involves the change of the optical phase in response to ultrasonic modulation of the optical index of refraction. The bottom line is that light transmitted through an organ contains different frequency components. The main carrier component is centered at the incident coherent optical beam frequency, whereas the sideband components are shifted by the ultrasound frequency. The intensity of the sideband, or "tagged," photons depends on the optical absorption in the region of interest. Demodulation of the optical speckle pattern yields the intensity of tagged photons for each location

of the ultrasonic focal spot. Thus one obtains an image with the spatial resolution of the focused ultrasound—typically submillimeter—whose contrast is related to local optical absorption and the diffusive properties of light in the organ. Fay Marks and colleagues were the first to investigate the ultrasonic light-modulation technique;² since their pioneering work in the early 1990s, many different groups have contributed to the field.³

The main difficulty in applying the technique to living tissues results from artifacts induced by the natural motions of blood flow and breathing. The resulting speckle decorrelation broadens the carrier and sideband lines. So, for example, when imaging a breast at a depth of 4 cm, the speckle decorrelation time is around a millisecond. The speckle pattern must therefore be frozen with better than millisecond quickness.

Although we have focused on acousto-optics, we also note that the tagging concept can be applied to other medical imaging modalities; one example is electric impedance tomography tagged by ultrasound-induced vibrations. Also worth noting is that magnetic resonance imaging, while not a multiwave approach, can be interpreted as a spatial-tagging technique. Magnetic resonance imaging uses a single RF electromagnetic wave with a wavelength of several meters. The spatial tagging is achieved with the help of a nonuniform static magnetic field that creates a spatially dependent Larmor relaxation frequency. An RF impulse transmitted into the organ causes protons to absorb a part of the impulse energy and release it later at the Larmor frequency. Thus, a frequency analysis of the received RF signal leads to a spatial resolution much smaller than the RF wavelength.

Wave-to-wave imaging

In the last example of multiwave imaging that we will consider, sonic shear waves and ultrasonic waves interact to yield a quantitative and highly resolved image of deep-organ stiffness, an important medical parameter often linked to pathology. Indeed, that link is the basis for the palpatory diagnosis of various diseases, such as in the detection of cancer nodules in the breast or prostate. Stiffness is characterized by Young's modulus $E = \tau/\zeta$, where τ is the stress (compression force per unit area) and ζ is the strain (fractional change in length).

Soft tissue is difficult to compress, but easy to shear. Consequently, the bulk modulus K , which characterizes how a tissue's volume changes in response to compression forces, is huge compared to the shear modulus μ , which quantifies how a tissue responds to shear forces. In that limit, the Young's and shear moduli are proportional to each other. As a result, the velocity c_s of a shear wave propagating through tissue with density ρ is simply related to Young's modulus: $c_s = \sqrt{\mu/\rho} = \sqrt{E/3\rho}$. An elegant way to access stiffness contrast in tissues, therefore, is to track the velocity of shear waves. Due to tissue's shear viscosity, however, shear waves can propagate only for some centimeters at the low sonic frequencies of 10–1000 Hz. Since a 100-Hz shear wave has a wavelength of several centimeters, single-wave imaging with shear waves leads to poor spatial resolution. Still, the stiffness contrast sensed by shear waves is important diagnostic information. Ultrasound, though it would provide better resolution, is not a good tool for finding stiffness-related pathologies because it propagates as a compression wave with an essentially uniform speed $c_p = \sqrt{K/\rho}$.

One way to get a stiffness image with a much better spatial resolution than shear waves alone can provide is to take a “wave-to-wave” approach that benefits from the huge dis-

Regimes of resolution

In conventional optical microscopy, the interrogating beam's wavelength controls the spatial resolution of an image, but such is not always the case. Indeed, three different regimes describe wave propagation through tissues: coherent, diffusive, and near-field. It is only in the coherent regime that wavelength determines resolution.

Ultrasonic waves, for example, can propagate tens of centimeters without losing their coherence. Since that distance is orders of magnitude greater than the typical wavelength of 0.1–1 mm, spatial resolution in ultrasound depends on the wavelength. In contrast, light at optical frequencies rapidly loses its coherence when propagating through opaque tissues and scattering off individual heterogeneities. More precisely, the light transport mean free path—about 1 mm—characterizes the distance after which light loses any memory of its initial direction. For applications like diffuse optical tomography (see the article by Arjun Yodh and Britton Chance in *PHYSICS TODAY*, March 1995, page 34), in which the propagation distance is much longer than the mean free path, the spatial resolution is on the order of the observation depth.

Most low-frequency electromagnetic imaging methods correspond to the near-field regime, in which the observation depth is much smaller than the wavelength. An example is electrical impedance tomography. With that technique, one generates low-frequency alternating currents at multiple electrodes placed on the skin and infers tissue conductivity from potential measurements at the electrodes. In the near-field regime, detectors sense the exponentially decaying evanescent waves radiated by a medium. The spatial resolution is on the order of the observation depth, independent of wavelength.

crepancy between shear and compression wave speeds. The idea is to use compression waves in the megahertz range—ultrasound, which has a speed of about 1500 m/s—to produce tissue images that follow the propagation of the relatively slow sonic shear waves with millimeter resolution. To do that with a typical shear-wave speed of 1–10 m/s requires a scanner that can capture up to 10 000 frames per second.

Our group developed such an ultrafast scanner,⁴ inspired in part by time-reversal mirrors (see reference 5 and the article by Mathias Fink in *PHYSICS TODAY*, March 1997,

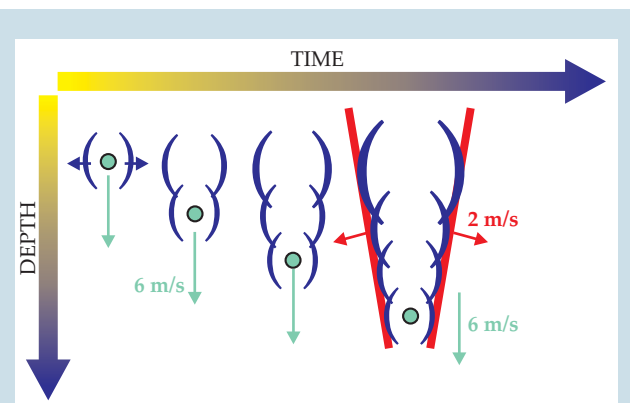


Figure 3. Supersonic shear generation. Bursts of ultrasound focused at successive depths in an organ each create a pushing force that induces a shear wave. When the source of the pushing force moves faster than the shear waves, the waves accumulate on a so-called Mach cone (red).

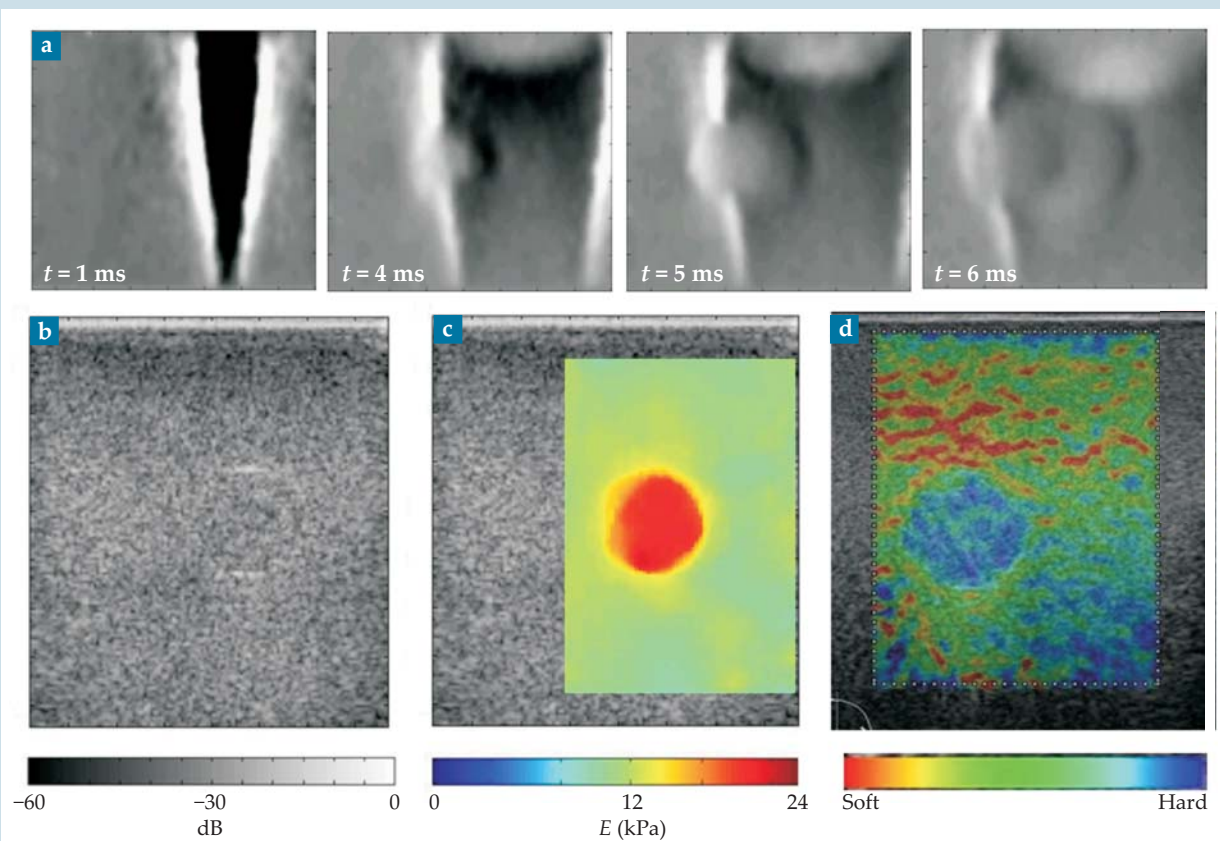


Figure 4. Supersonic shear-wave imaging. (a) These four frames are from an ultrasound movie of local displacements in a tissue-mimicking material (a “phantom”) at specified times after the supersonic generation of a shear wave. The gray scale indicates displacements from $-10 \mu\text{m}$ to $+10 \mu\text{m}$. Clearly, the shear wave is sensing the stiffness contrast as it is distorted while passing through a 10-mm-diameter stiff inclusion. (b) A conventional ultrasonic image of the medium barely reveals the inclusion. (c) From the movie sampled in panel a, one can obtain a quantitative image of Young’s modulus E . (d) An image of the same phantom as in panel c, obtained with a commercially available ultrasound scanner using static elastography, a single-wave approach discussed in the text.

page 34). For our ultrafast imaging, an array of some hundreds of piezoelectric transducers transmits an ultrasonic beam spread over the whole area of interest and, at several thousand times per second, records the resulting backscattered echoes in large memories. Because the speed of an ultrasonic wave is known and constant, the data can rapidly be transformed into an image through numerical time-reversal refocusing. Our procedure is very different from that used with conventional ultrasound scanners that probe the medium using only a very thin ultrasonic beam that is translated step by step to map the imaged area. As highlighted in figure 1, conventional ultrasound typically requires some hundreds of ultrasonic bursts to produce a single image; our technique produces an image from each ultrasonic transmission.

The tracking of local displacements induced by shear-wave propagation requires a comparison of successive ultrasonic images. Such a procedure is possible because each frame is dominated by an ultrasonic speckle pattern that, like optical speckle, originates from the random distribution of scatterers that exist everywhere in tissues. But unlike light scattering, ultrasonic backscattering in soft tissue is dominated by a single scattering process. Thus the arrival time of the speckle noise corresponds to a specific spatial location of the scatterers. By correlating in time the speckle noise observed from one frame to the next, a “speckle tracking” algo-

rithm enables the estimation of local tissue displacements along the ultrasonic beam direction. From that sequence, one can deduce the local shear-wave speed and thus the Young’s modulus.

But how are the shear waves generated in the human body to begin with? First, note that shear waves exist naturally in our bodies: Heartbeats, for example, create transient vibrations that propagate near the cardiac muscles and along arteries. Artificially induced shear waves can arise from carefully controlled external vibrators applied at the surface of the body. A perhaps more elegant way was proposed by Armen Sarvazyan and colleagues in 1998.⁶ The idea is to focus an ultrasonic beam at a given depth in the organ with an array of transducers to create a radiation force localized in the focal spot and oriented along the beam axis. That force—due to the momentum transfer from the ultrasonic wave to the medium caused by nonlinearities, dissipation, and reflection—is proportional to the square of the ultrasound pressure field. Typically, it leads to a low-frequency axial displacement of some tens of microns at several centimeters’ depth. Once the ultrasonic burst ends, tissue displaced in the focal spot comes back to its equilibrium position and thus generates a localized source of shear waves. Figures 2a and 2b illustrate the process. Panels 2c and 2d show examples of the frames that are produced when the ultrasonic array switches to its ultrafast

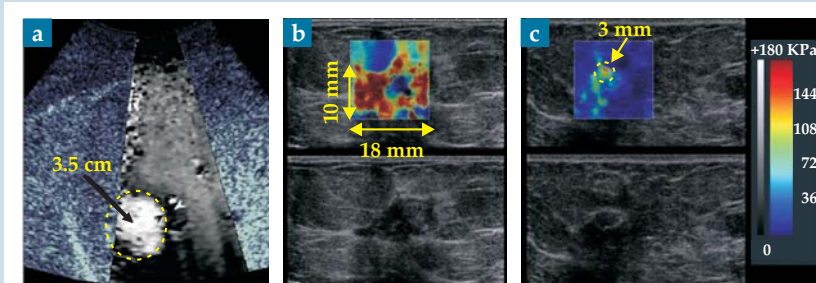


Figure 5. Tumors revealed by acoustic radiation force impulse imaging and supersonic shear-wave imaging. **(a)** A liver tumor is obtained with ARFI imaging. The gray scale indicates relative displacement. The white region shows the 3.5-cm-diameter soft tumor. (Adapted from ref. 12.) **(b)** Two-dimensional, high-resolution color map of Young's modulus of a breast. The image, obtained using supersonic shear-wave imaging, is superimposed on a conventional ultrasonic image. Clearly visible in the color map is an invasive ductal carcinoma. It presents a stiff boundary (red) surrounding a soft 5-mm core (blue) that corresponds to a necrotic region. Histology confirmed the presence of the necrotic area. **(c)** The color map here, also obtained with supersonic shear-wave imaging, reveals two very small lesions that escaped detection by x-ray mammography. (Images in panels b and c courtesy of SuperSonic Imagine.)

imaging mode to film the shear-wave propagation.

The amplitude of the radiated shear wave decreases rapidly due to the natural divergence associated with a small shear-wave source. To extend the area sensed by the shear wave, we teamed up with J  r  my Bercoff to propose a supersonic shear source.⁷ By changing the electronic delays between the signals transmitted by transducer elements, one can create long bursts of ultrasonic waves successively focused at different focal depths, as illustrated in figure 3. If the resulting shear-wave source moves faster than the radiated shear waves, constructive interference along a Mach cone will yield high-displacement shear waves that can travel over relatively long distances. That sonic boom is a mechanical analogue to the Cherenkov radiation emitted by a beam of high-energy charged particles passing through a transparent medium at a speed greater than the medium's speed of light.⁸

Our group tested the supersonic shear-wave source idea with an experiment conducted on a material that mimics tissue. As figure 4 shows, a conventional ultrasonic image of the tissue-mimicking phantom indicates an almost perfectly homogeneous bulk modulus, even though the phantom contains a stiffer inclusion with a diameter of 10 mm. Much more revealing are high-frame-rate ultrasonic images of tissue displacements recorded after the shear wave is radiated by the supersonic source. Evidently, the shear wave, which accelerates through the stiffer inclusion, is sensitive to Young's modulus.

The resolution of the Young's modulus map in figure 4c is about a millimeter, even though the wavelength of the shear wave is about a centimeter. Such superresolution ultimately arises because the local displacements induced by the wave propagation are recorded not only on the boundaries of the investigated medium—for example, as in seismology—but at numerous locations deep in the investigated medium. Thus, the wave-to-wave approach provides information about the near field of the shear waves around each inhomogeneity.

Other elasticity imaging methods

In parallel with wave-to-wave approaches that use ultrafast ultrasound scanners, the quest for stiffness imaging has seen

extensive research on techniques that use conventional ultrasound scanners with frame rates of less than 50 frames/s. The concept of stiffness imaging was introduced in the early 1990s by Jonathan Ophir and company, who called their method "elastography."⁹ To apply their single-wave technique, an operator manipulates a handheld ultrasonic probe at the surface of a subject's body to induce a static compression of the subject's organs. After acquiring precompression and post-compression ultrasound images, the operator can obtain the tissue deformation.

More precisely, the image comparison yields an elastogram, a map of local tissue strain. Because soft regions tend to exhibit a higher strain than stiffer areas, the strain is linked to stiffness—that is, to Young's modulus. But the link is dependent on a local, unknown stress and, unfortunately, the compression applied at

the body surface can create a complex spatial distribution of stress that induces image artifacts. The effect can be seen in figure 4d in the strong heterogeneities that appear close to the hard inclusion.

In 2001 Kathryn Nightingale and colleagues proposed a second elasticity imaging technique, acoustic radiation force impulse (ARFI) imaging.¹⁰ Like the wave-to-wave approach discussed above, ARFI exploits a radiation force induced by a focused ultrasound beam. Tissue displacements, however, can be measured only at the location of the focal spot because the limited frame rate of conventional ultrasound scanners does not allow real-time tracking of the radiated shear wave. A complete image can be generated by steering the focal spot to different locations. Moreover, as with the static elastography introduced by Ophir, ARFI imaging yields a strain image; the local stress needed to deduce Young's modulus remains unknown.

Because ARFI does not follow the radiated shear wave in real time, it is not a multiwave approach. The technique of magnetic resonance (MR) elastography, introduced by Raja Muthupillai and colleagues in 1995, is a multiwave modality.¹¹ In its application, vibrators on the surface of a subject's body continuously generate a shear wave. Magnetic resonance then enables three-dimensional imaging of tissue displacements that occur in response to the propagating shear wave. Thanks to its multiwave nature, MR elastography provides after several minutes' acquisition time a quantitative image of Young's modulus with a millimeter resolution.

All the elastography techniques we have discussed are currently under extensive clinical evaluation^{12,13} and are beginning to be commercialized. Figure 5 shows some of those studies' results. Panel 5a shows an *in vivo* ARFI strain image of a 35-mm-diameter liver tumor superimposed on a conventional ultrasonic image. The large displacements visible in the figure are typical for primary liver cancer, which tends to be softer than surrounding tissues. Panels 5b and 5c show *in vivo* images generated with the help of supersonic shear-wave imaging. They reveal breast cancer tumors with millimeter resolution.

Multiwave imaging is now a fertile field from which new ideas and technologies are emerging. It has, for example, pro-

vided a way to observe with far-field detectors the near field of waves around heterogeneities. The approach is particularly useful for obtaining three physical parameters that until recently have been difficult to map with good spatial resolution: optical absorption, electrical conductivity, and Young's modulus. We believe that multiwave imaging, like molecular imaging, has a bright future in the field of medicine. Already, elasticity imaging has to its credit significant clinical success in cancer diagnosis. The commercial successes that we see on the horizon for multiwave imaging will be the best proof of the technique's utility.

References

1. B. C. Towe, M. R. Islam, *IEEE Trans. Biomed. Eng.* **35**, 892 (1988); X. Li, Y. Xu, B. He, *J. Appl. Phys.* **99**, 066112 (2006).
2. F. A. Marks, H. W. Tomlinson, G. W. Brooksby, in *Photon Migration and Imaging in Random Media and Tissues*, B. Chance, R. R. Alfano, eds., SPIE, Bellingham, WA (1993), p. 500.
3. See, for example, L. Wang, S. L. Jacques, X. Zhao, *Opt. Lett.* **20**, 629 (1995); W. Leutz, G. Maret, *Physica B* **204**, 14 (1995); S. Lévesque et al., *Opt. Lett.* **24**, 181 (1999).
4. L. Sandrin et al., *IEEE Trans. Ultrason. Ferroelectr. Freq. Control* **49**, 426 (2002).
5. M. Fink, G. Montaldo, M. Tanter, *Annu. Rev. Biomed. Eng.* **5**, 465 (2003).
6. A. P. Sarvazyan et al., *Ultrasound Med. Biol.* **24**, 1419 (1998).
7. J. Bercoff, M. Tanter, M. Fink, *IEEE Trans. Ultrason. Ferroelectr. Freq. Control* **51**, 396 (2004).
8. J. Bercoff, M. Tanter, M. Fink, *Appl. Phys. Lett.* **84**, 2202 (2004).
9. J. Ophir et al., *Ultrason. Imaging* **13**, 111 (1991).
10. K. Nightingale et al., *J. Acoust. Soc. Am.* **110**, 625 (2001).
11. R. Muthupillai et al., *Science* **269**, 1854 (1995).
12. B. J. Fahey et al., *Phys. Med. Biol.* **53**, 279 (2008).
13. A. Itoh et al., *Radiology* **239**, 341 (2006); S. K. Venkatesh et al., *Am. J. Roentgenol.* **190**, 1534 (2008); M. Tanter et al., *Ultrasound Med. Biol.* **34**, 1373 (2008). ■

MAGNETS

NEODYMIUM IRON BORON • SAMARIUM COBALT
CERAMIC • ALNICO
MAGNETIC ASSEMBLIES • COMPLETE DESIGN FACILITIES



With a state of the art manufacturing facility which is certified to **SAE AS 9100B** and **ISO 9001:2000** we can deliver a quality magnet, assembly or subassembly **fast**. MCE can also fully engineer and design a solution for your magnet requirement. Call, fax or visit our web site www.mceproducts.com for an **immediate** quotation.



MAGNETIC COMPONENT ENGINEERING, INC.

2830 Lomita Blvd. • Torrance, CA 90505

Toll Free: 800-989-5656 • Main: 310-784-3100 • Fax: 310-784-3192

E-mail: mcesales@mceproducts.com Website: www.mceproducts.com

XRF Solutions

- Solid State Design
- Easy to Use

Complete XRF System



- No Liquid Nitrogen!!
- USB Controlled

Complete X-Ray Spectrometer



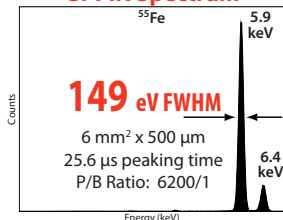
- Thermoelectric Cooler
- Low Cost

OEM Components

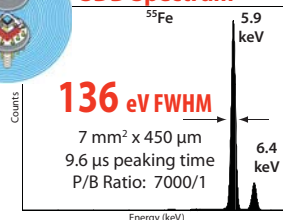


Your choice of Si-PIN Detector or Silicon Drift Detector or CdTe-diode Detector

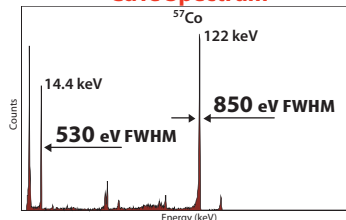
Si-PIN Spectrum



SDD Spectrum



CdTe Spectrum



OEM's #1 Choice
for XRF



AMPTEK Inc. 14 DeAngelo Drive, Bedford, MA 01730-2204 USA

Tel: +1 781 275-2242 Fax: +1 781 275-3470 E-mail: sales@amptek.com

www.amptek.com